deep run®

lowtech solution

Engineering Services for Marine Renewable Energies and Offshore applications

DEEPRUN team

Matthieu HOARAU
Founder & President
14 years of experience
Entrepreneurship & project management
Expert in **Marine Renewable Energies**

Lucas VATINEL
Naval engineer
3 years of experience
Specialized in **Hydrodynamics**

Ludovic MOUTIEN
Structure engineer
12 years of experience in aeronautics
Specialized in **Structures**

DEEPRUN partners

deep run lowtech solution

UNIVERSITÉ DE LA RÉUNION

ENSTA Bretagne

aiRaRo

ENERGY LAB

Ifremer

INNOSEA
An LOC Group company

IUT DE LA RÉUNION
Institut Universitaire de Technologie

UNIVERSITÉ DE LORRAINE

Ansys
STARTUP PROGRAM

Liberté • Égalité • Fraternité
RÉPUBLIQUE FRANÇAISE
MINISTÈRE
DE L'ENSEIGNEMENT SUPÉRIEUR,
DE LA RECHERCHE
ET DE L'INNOVATION

ADEME
AGENCE DE LA TRANSITION ÉCOLOGIQUE

bpifrance

TECHNOPOLE DE LA RÉUNION

Initiative Réunion
ENTREPRENDRE

REGION RÉUNION
www.regionreunion.com

Liberté • Égalité • Fraternité
RÉPUBLIQUE FRANÇAISE

DEEPRUN engineering

Hydrodynamic & Structural engineering

Complex Numerical engineering

Standards checking

Mechanical testing

Technical reporting

Agile project development

Hydrodynamics engineering

➢ Expertise:

- Specific environments analysis, determination and implementation in numerical models *(waves (various linearity, regularity), current, extreme conditions, …)*
- Complex system behavior characterization and modelling *(Morison forces, pressure loads, dynamic constraints, …)*
- Tailored numerical models' development *(Equation solving, code development & validation)*
- Analytical model development

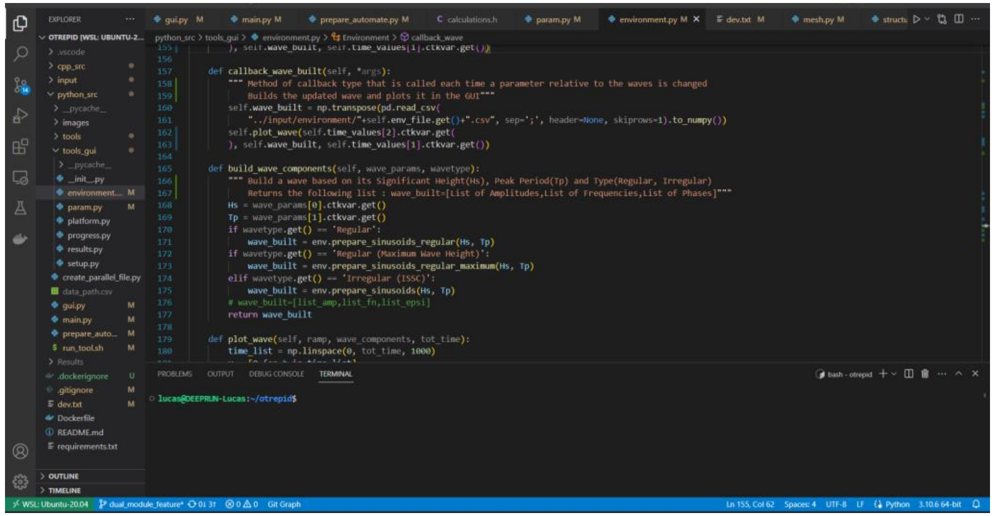

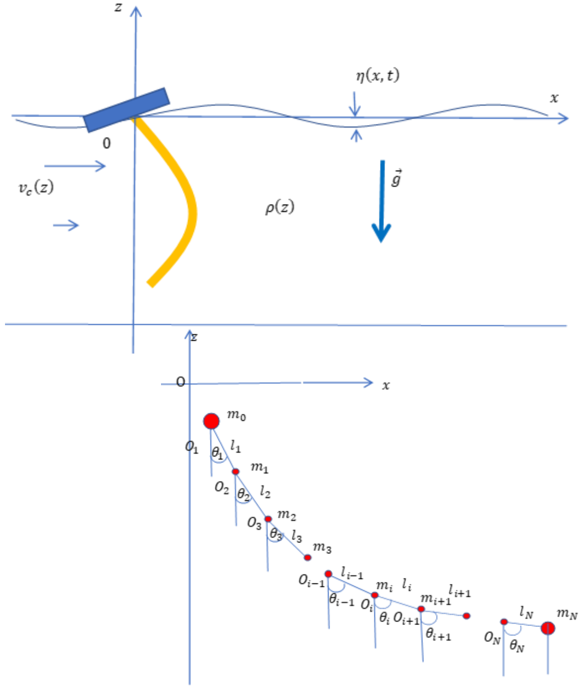

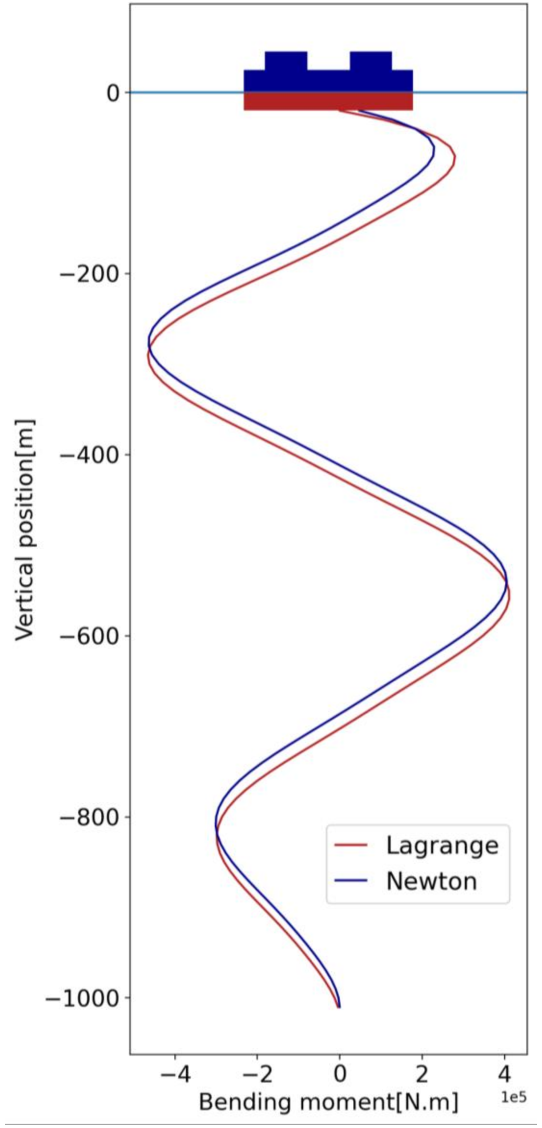

➢ Site characterization :

- Global database management
- Environmental databases compilation
- Specific site environmental conditions characterization

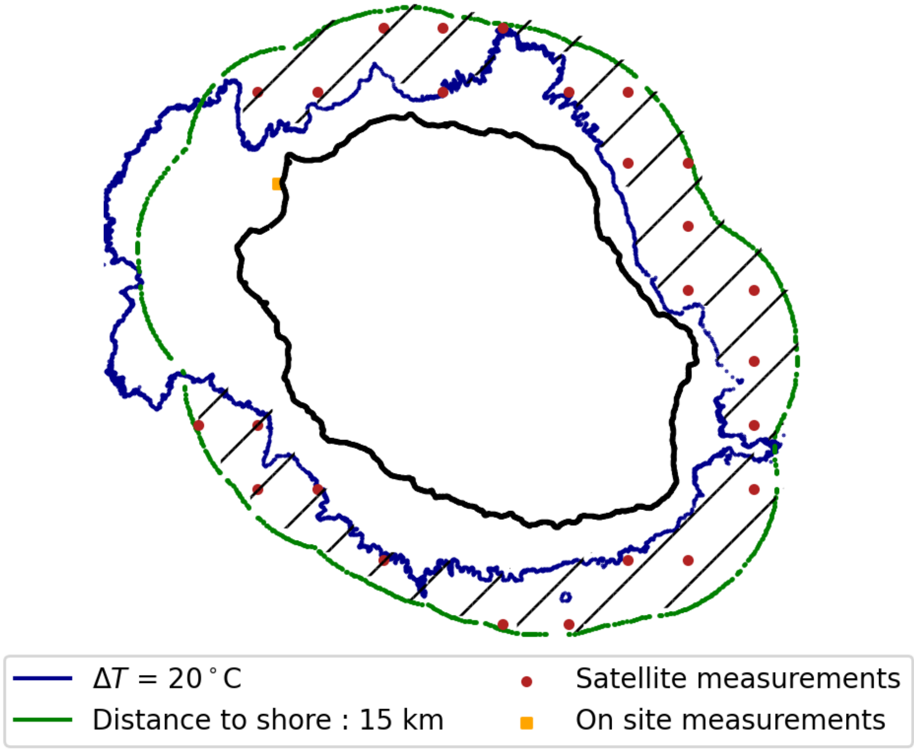

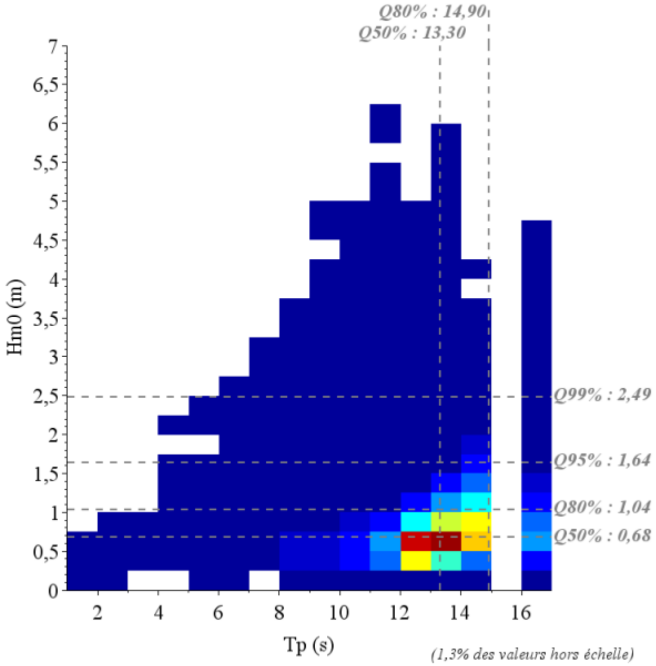

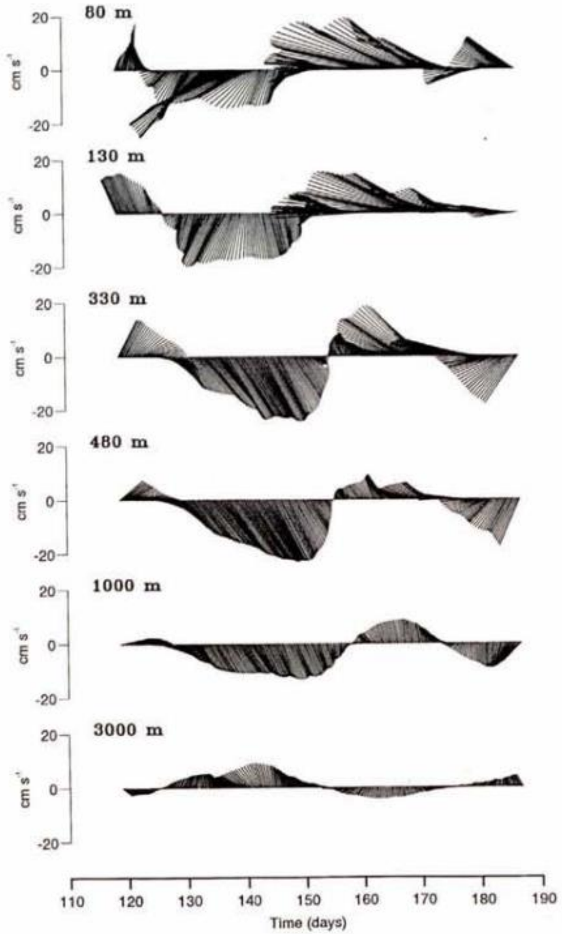

➢ Complex structural calculations:

- Loads and stresses distribution in complex assembly
- Static and fatigue strengths of assembly
- Material and buckling behavior determination

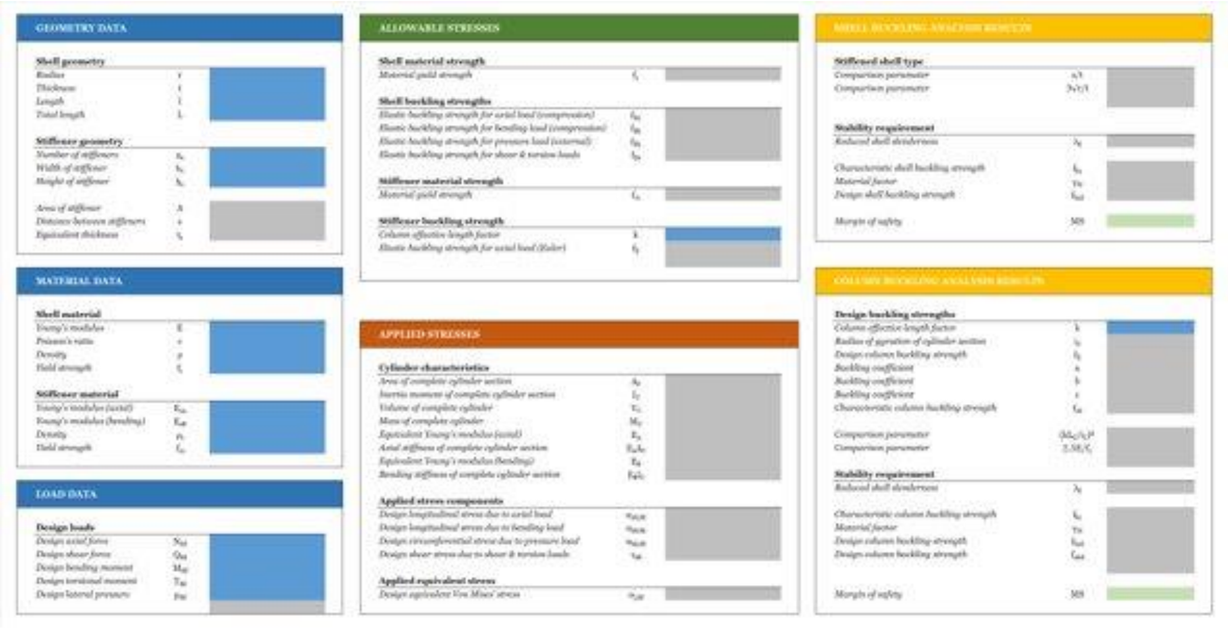

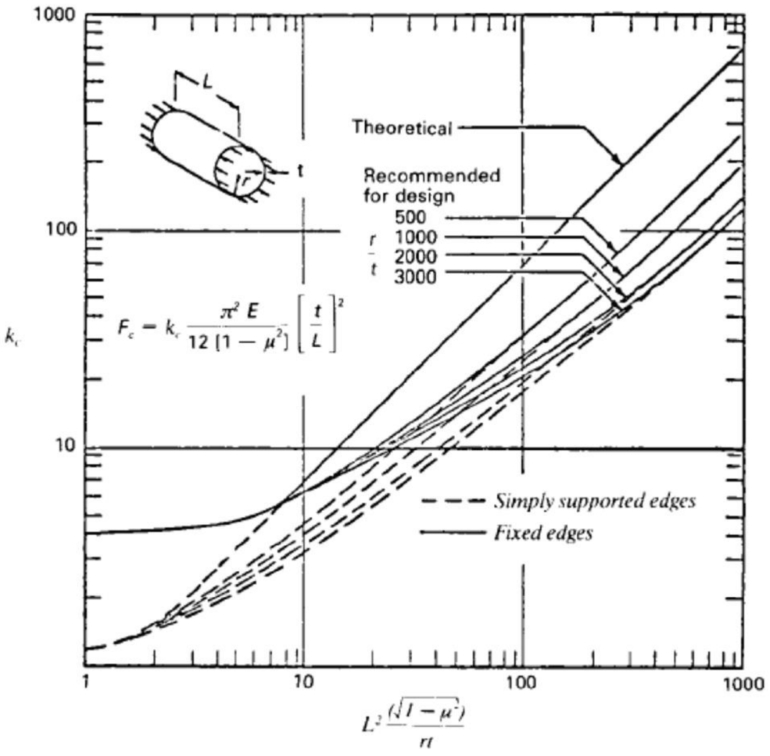

Numerical engineering

➢ <u>Structural engineering with finite element software on complex and multi-material assembly :</u>

- Finite element modeling
- Load path analysis
- Static analysis
- Linear buckling analysis
- Fatigue analysis

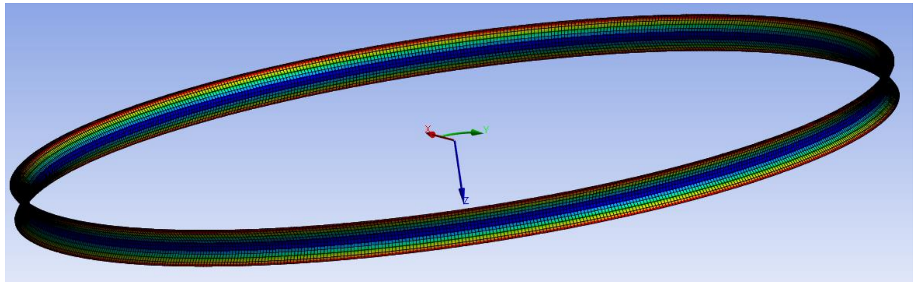

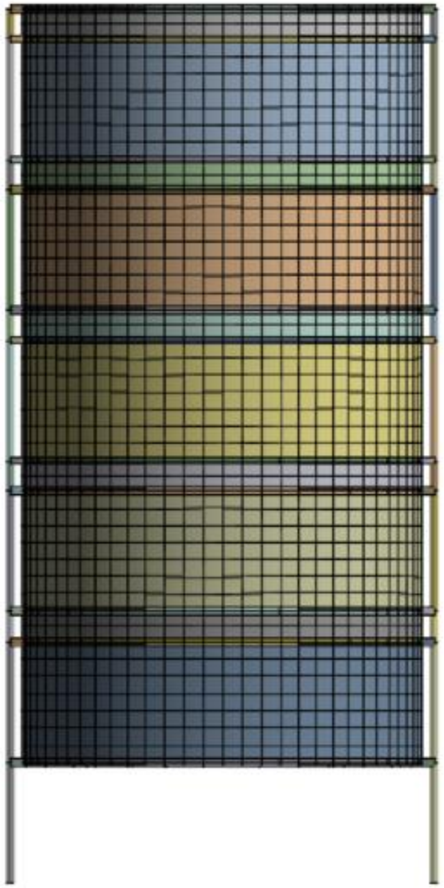

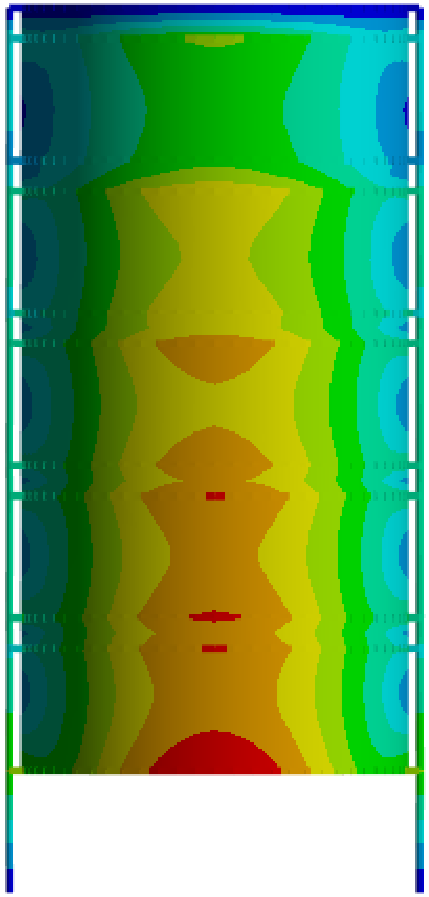

Numerical analyses

➢Development of in-house and tailored Human Machine Interface tool for hydrodynamic analyses

- Complex numerical tools implementation
- Fast calculation kernel in C++
- Pre- and Post-processing in Python

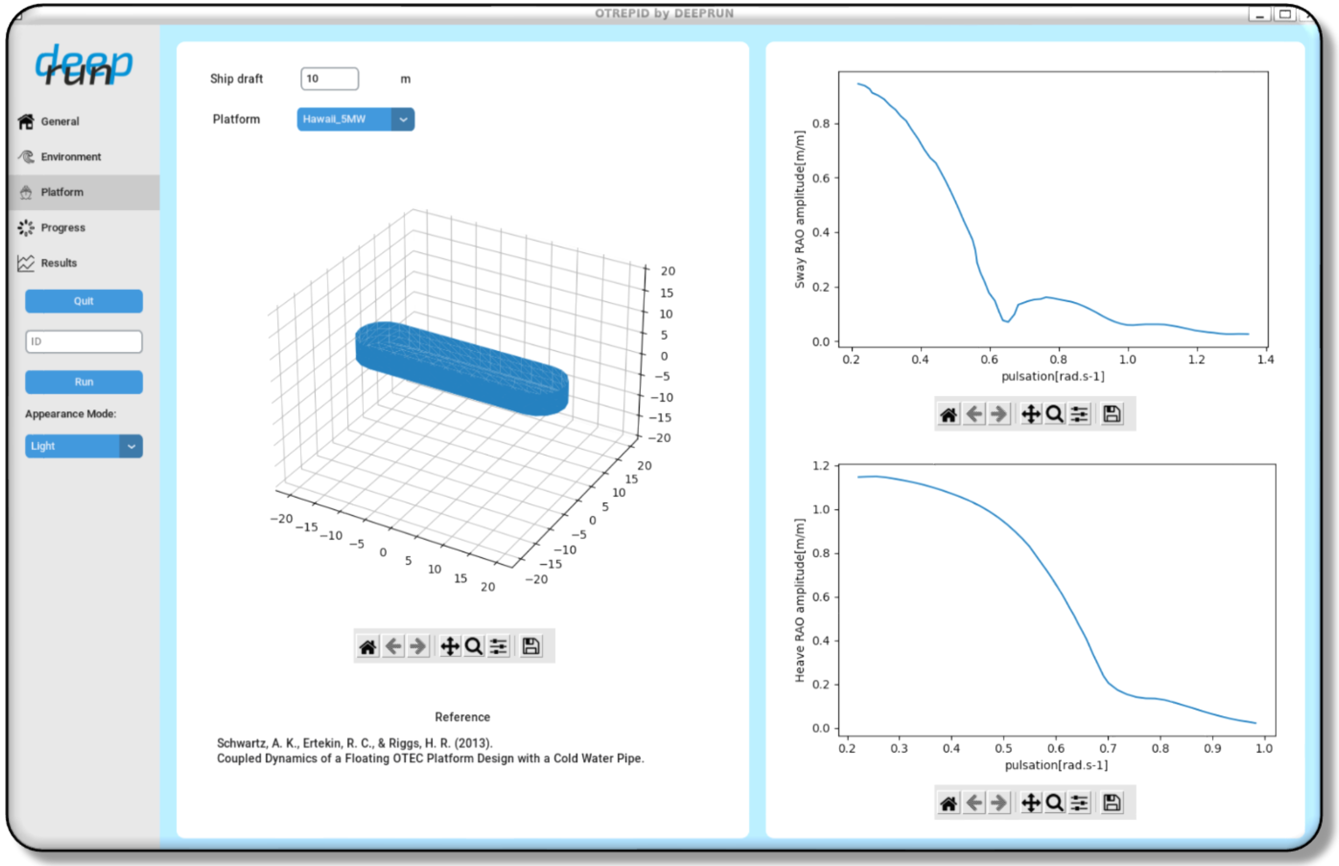

Standards checking

➢ Implementation and application of DNV rules:

- Determination of environmental conditions
- Determination of hydrodynamic coefficients
- Verification of structural requirements
- Analyses with certified structural methods

➢ Implementation and application of Eurocode standards:

- Eurocode 3 for stability and strength of structures
- Eurocode 5 for strengths of connections

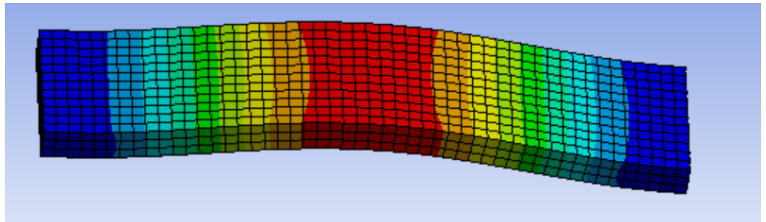

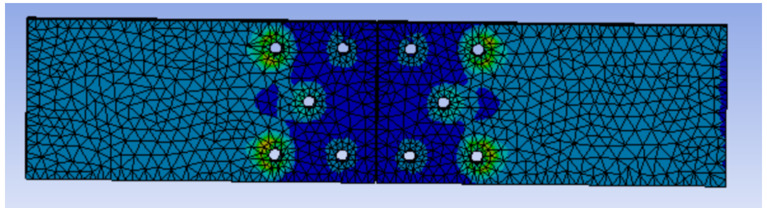

➢ Specific and dedicated mechanical tests :

- Tensile/compressive/bending tests with different materials
- Mechanical properties to be correlated in analyses

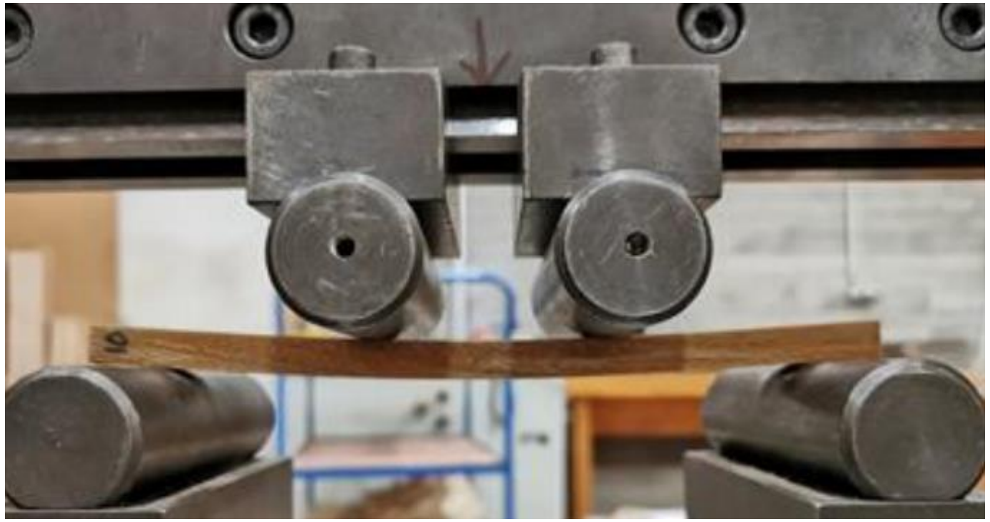

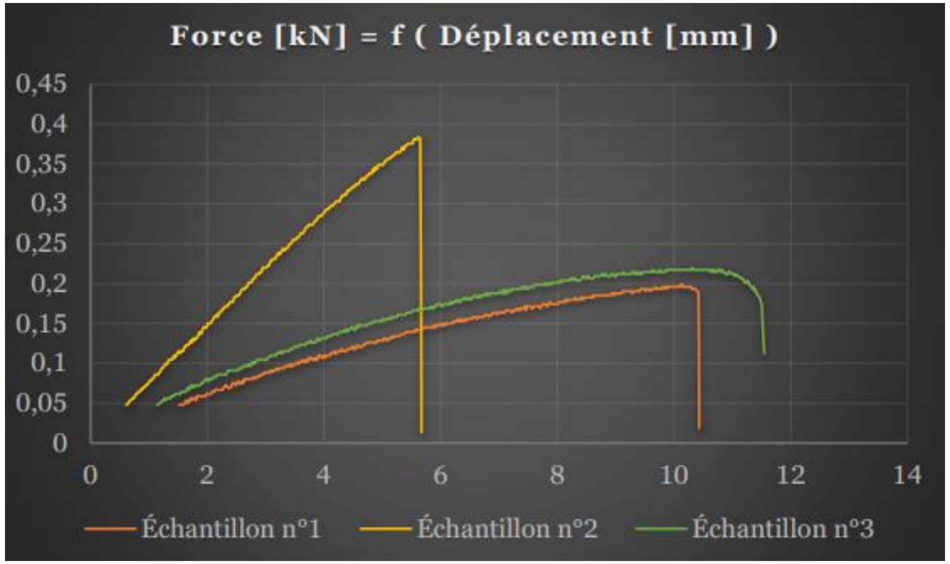

Mechanical testing

➢ <u>Bending tests on small-scale prototype:</u>

- Definition of tests adapted to tests means and prototypes
- Design and analysis of small scale prototype
- Manufacturing of custom-designed parts and connections

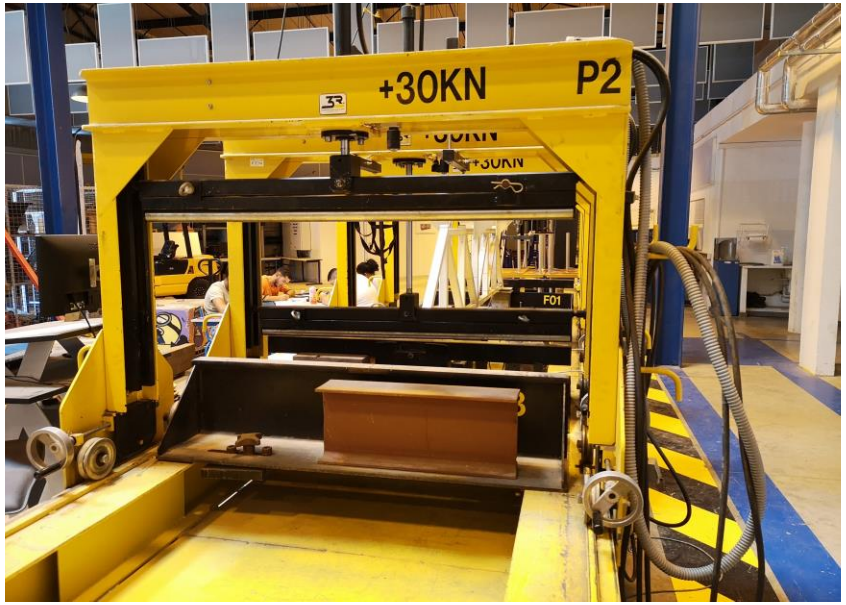

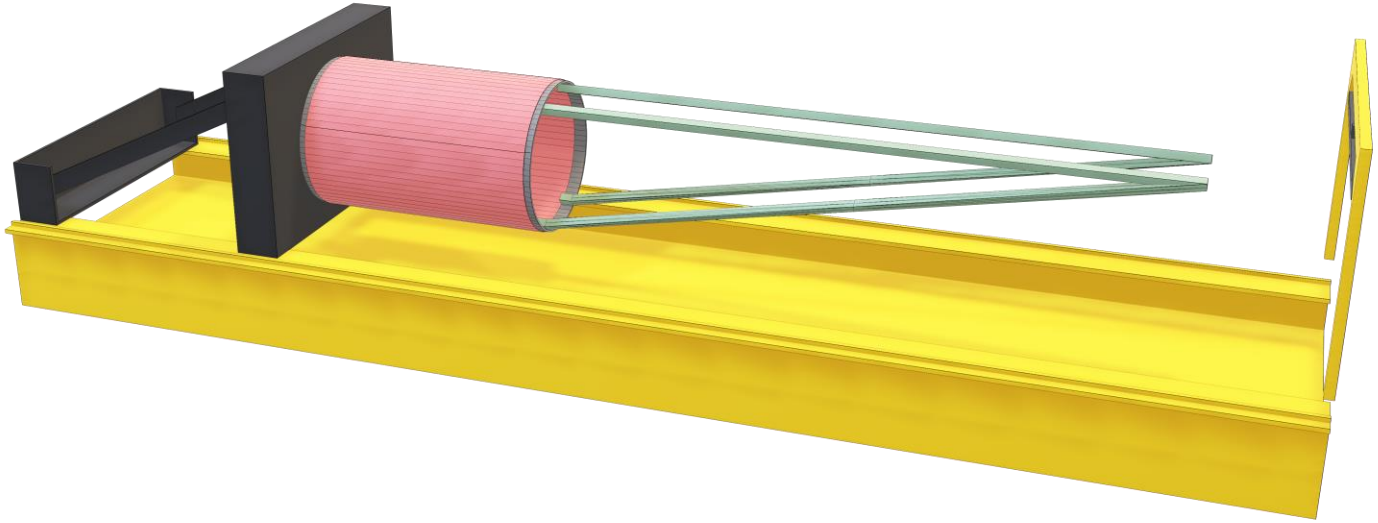

Technical reporting

➢Analysis reports

These parameters are used as input in the cPendulum pipe model, as well as the wave elevation and the current velocity. The cPendulum simulation gives the motion of the pipe as a result, as well as the forces related.

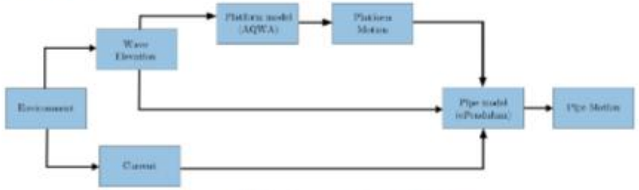

Figure 2.3: Hydrodynamic study method chart

2.2.2 Ansys AQWA model

The platform model is mandatory to design the pipe, however DEEPRUN's intention is not to design the platform. In the future, the client would provide the 3D of the platform, its mooring lines and maybe its RAOs, so that DEEPRUN focus on the pipe.

The aim of the AQWA model is to simulate a physical motion of an OTEC floating platform. The model is shown previously in Figure 1.1. It is simply composed with a floating platform moored by four catenary lines.

Mooring Lines The mooring lines, whose characteristics are summed up in Table 2.1, have been designed to resist to the following cyclonic conditions :

- wind speed of $70m.s^{-1}$
- current velocity of $0.4m.s^{-1}$
- irregular swell based on ISSC Spectrum with a significant wave height of 6m and a peak period of 13s

Line Characteristics	Values	Unit
Chain Link Diameter	140	mm
Linear Mass	341	kg/m
Suspended Length	2368	m
Length to Touchdown Point	859	m
Transversal Drag Coefficient	3.5	-
Longitudinal Drag Coefficient	1.7	-
Proof Load	11186	kN

Table 2.1: Mooring line characteristics

The added mass and drag coefficients of the mooring line have been determined using DNV rules, and take into account the marine growth.

The tension in the line is compared to the proof load of the chain following DNG-GL-OS-E301 [3], and for both ULS[3] and ALS[4], the safety ratio is below 1, which validates the choice of the lines.

[3]Ultimate Limit States
[4]Accidental Limit States

Floating Platform The main floating platform's dimensions and its hull mesh are shown in the figure 2.4.

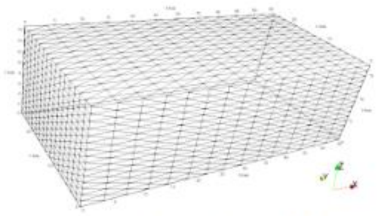

Dimension	Values	Unit
Length	56	m
Width	26	m
Depth	23	m
Draft	16.5	m
Displacement	23 000	tons

Figure 2.4: Platform's hull mesh and main dimensions

The hull is about twice as long as it is wide, therefore the direction that has the biggest area subject to environmental forces is the Y direction defined in the Figure 2.4. The considered direction for the designing environmental forces is then the Y direction.

In these conditions, the degrees of freedom having a significant motion are sway, heave and roll. However, as the link between the pipe and the platform is assumed to be a mechanical ball joint, the degrees of freedom impacting the motion of the pipe are therefore sway and heave.

The motion of the platform used as input for the determination of the pipe's motions is calculated under the operational wave conditions expressed in 2.1.3 ($H_{m0} = 3m$ and $T_p = 13s$). An exemple of sway and heave of the platform under randomly generated irregular waves is shown in Figure 2.5.

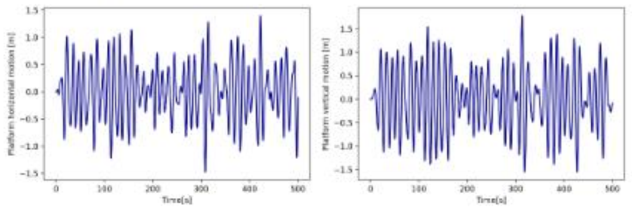

(a) Sway (b) Heave

Figure 2.5: Platform motion under irregular waves

2.2.3 cPendulum model

The motion of the pipe is calculated over time using the in-house code cPendulum. The pipe is modelled and discretised as a series of masses attached to each other.

➢ Test reports

1.4. Résultats prise de masse volumique

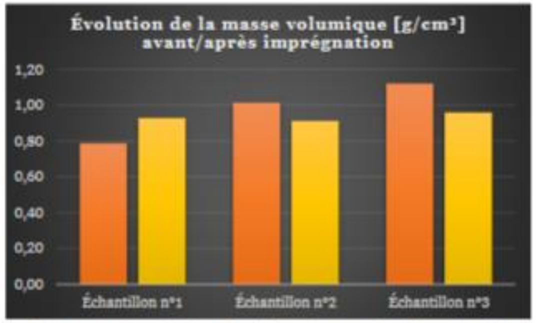

Figure 3 : Masses volumiques des échantillons avant/après imprégnation

	ρ_{av} [g/cm³]	ρ_{ap} [g/cm³]	Prise de masse volumique [%]
N°1	0,79	0,93	+17,74
N°2	1,01	0,91	-9,99
N°3	1,12	0,96	-14,38
Moyenne	**0,97**	**0,93**	**-2,21**
Écart type	**0,17**	**0,02**	**17,42**

Tableau 5 : Résultats prise de masse volumique des échantillons

Vu les résultats précédents sur le gonflement, l'analyse de l'évolution de la masse volumique des échantillons avant et après imprégnation est délicate :

- D'une part, par rapport aux écarts qu'on note sur les masses volumiques avant imprégnation. On aurait pu s'attendre à une homogénéité des valeurs sur tous les échantillons.
- D'autre part, par rapport à l'incohérence entre un taux d'imprégnation à l'eau homogène et très faible, et une prise de volume assez marquée et hétérogène.

Il en résulte forcément des valeurs très différentes (Écart type > 15) avec des comportements contraires. Il est donc impossible de dégager une tendance comme précédemment avec le taux d'imprégnation.

2. Essais de flexion à l'Université de Lorraine (Nancy-Epinal)

2.1. Dispositif de l'essai en flexion

Les tests mécaniques ont été réalisés en utilisant un dispositif de flexion 4 points :

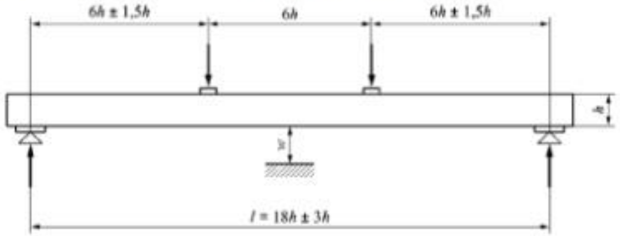

Figure 4 : Dispositif d'essai pour mesurer les caractéristiques en flexion

Les figures suivantes illustrent le dispositif d'essai utilisé pour la flexion 4 points :

Figure 5 : Photographie de l'INSTRON 4206 utilisé pour l'essai en flexion 4 points

Figure 6 : Photographie du logiciel de commande et enregistrement des mesures

deep run lowtech solution

➢Scientific publications

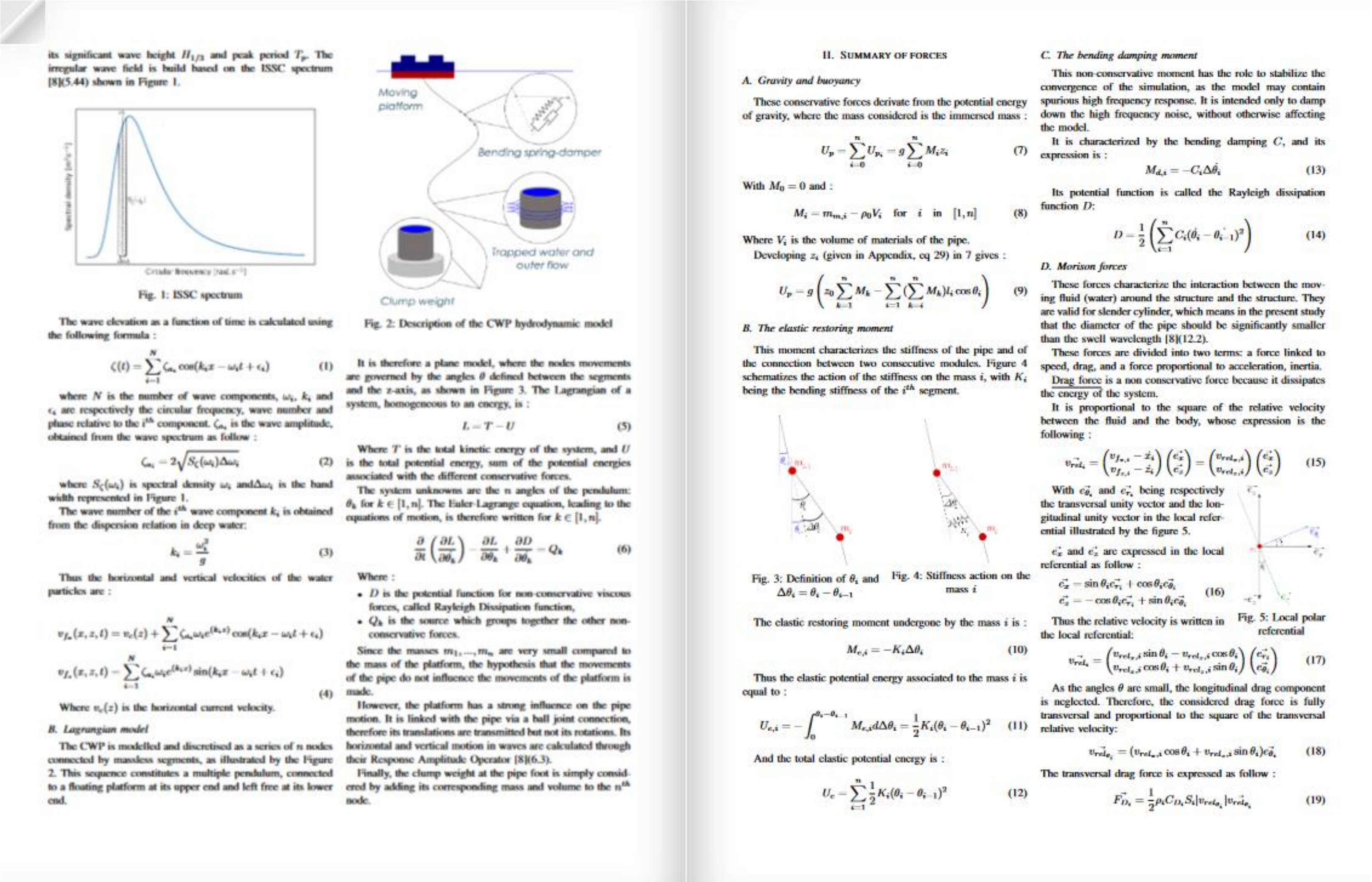

its significant wave height $H_{1/3}$ and peak period T_p. The irregular wave field is build based on the ISSC spectrum [8](5.44) shown in Figure 1.

Fig. 1: ISSC spectrum

The wave elevation as a function of time is calculated using the following formula :

$$\zeta(t) = \sum_{i=1}^{N} \zeta_{a_i} \cos(k_i x - \omega_i t + \epsilon_i) \quad (1)$$

where N is the number of wave components, ω_i, k_i and ϵ_i are respectively the circular frequency, wave number and phase relative to the i^{th} component. ζ_{a_i} is the wave amplitude, obtained from the wave spectrum as follow :

$$\zeta_{a_i} = 2\sqrt{S_\zeta(\omega_i)\Delta\omega_i} \quad (2)$$

where $S_\zeta(\omega_i)$ is spectral density ω_i and$\Delta\omega_i$ is the band width represented in Figure 1.

The wave number of the i^{th} wave component k_i is obtained from the dispersion relation in deep water:

$$k_i = \frac{\omega_i^2}{g} \quad (3)$$

Thus the horizontal and vertical velocities of the water particles are :

$$v_{f_x}(x,z,t) = v_c(z) + \sum_{i=1}^{N} \zeta_{a_i}\omega_i e^{(k_i z)} \cos(k_i x - \omega_i t + \epsilon_i)$$
$$v_{f_z}(x,z,t) = \sum_{i=1}^{N} \zeta_{a_i}\omega_i e^{(k_i z)} \sin(k_i x - \omega_i t + \epsilon_i) \quad (4)$$

Where $v_c(z)$ is the horizontal current velocity.

B. Lagrangian model

The CWP is modelled and discretised as a series of n nodes connected by massless segments, as illustrated by the Figure 2. This sequence constitutes a multiple pendulum, connected to a floating platform at its upper end and left free at its lower end.

Moving platform
Bending spring-damper
Trapped water and outer flow
Clump weight

Fig. 2: Description of the CWP hydrodynamic model

It is therefore a plane model, where the nodes movements are governed by the angles θ defined between the segments and the z-axis, as shown in Figure 3. The Lagrangian of a system, homogeneous to an energy, is :

$$L = T - U \quad (5)$$

Where T is the total kinetic energy of the system, and U is the total potential energy, sum of the potential energies associated with the different conservative forces.

The system unknowns are the n angles of the pendulum: θ_k for $k \in [1,n]$. The Euler-Lagrange equation, leading to the equations of motion, is therefore written for $k \in [1,n]$.

$$\frac{\partial}{\partial t}\left(\frac{\partial L}{\partial \dot\theta_k}\right) - \frac{\partial L}{\partial \theta_k} + \frac{\partial D}{\partial \dot\theta_k} = Q_k \quad (6)$$

Where :

- D is the potential function for non-conservative viscous forces, called Rayleigh Dissipation function,
- Q_k is the source which groups together the other non-conservative forces.

Since the masses $m_1, ..., m_n$ are very small compared to the mass of the platform, the hypothesis that the movements of the pipe do not influence the movements of the platform is made.

However, the platform has a strong influence on the pipe motion. It is linked with the pipe via a ball joint connection, therefore its translations are transmitted but not its rotations. Its horizontal and vertical motion in waves are calculated through their Response Amplitude Operator [8](6.3).

Finally, the clump weight at the pipe foot is simply considered by adding its corresponding mass and volume to the n^{th} node.

II. SUMMARY OF FORCES

A. Gravity and buoyancy

These conservative forces derivate from the potential energy of gravity, where the mass considered is the immersed mass :

$$U_p = \sum_{i=0}^{n} U_{p_i} = g\sum_{i=0}^{n} M_i z_i \quad (7)$$

With $M_0 = 0$ and :

$$M_i = m_{m,i} - \rho_0 V_i \quad \text{for} \quad i \quad \text{in} \quad [1,n] \quad (8)$$

Where V_i is the volume of materials of the pipe.

Developing z_i (given in Appendix, eq 29) in 7 gives :

$$U_p = g\left(z_0\sum_{k=1}^{n} M_k - \sum_{i=1}^{n}(\sum_{k=i}^{n} M_k) l_i \cos\theta_i\right) \quad (9)$$

B. The elastic restoring moment

This moment characterizes the stiffness of the pipe and of the connection between two consecutive modules. Figure 4 schematizes the action of the stiffness on the mass i, with K_i being the bending stiffness of the i^{th} segment.

Fig. 3: Definition of θ_i and $\Delta\theta_i = \theta_i - \theta_{i-1}$

Fig. 4: Stiffness action on the mass i

The elastic restoring moment undergone by the mass i is :

$$M_{e,i} = -K_i \Delta\theta_i \quad (10)$$

Thus the elastic potential energy associated to the mass i is equal to :

$$U_{e,i} = -\int_0^{\theta_i - \theta_{i-1}} M_{e,i} d\Delta\theta_i = \frac{1}{2}K_i(\theta_i - \theta_{i-1})^2 \quad (11)$$

And the total elastic potential energy is :

$$U_e = \sum_{i=1}^{n}\frac{1}{2}K_i(\theta_i - \theta_{i-1})^2 \quad (12)$$

C. The bending damping moment

This non-conservative moment has the role to stabilize the convergence of the simulation, as the model may contain spurious high frequency response. It is intended only to damp down the high frequency noise, without otherwise affecting the model.

It is characterized by the bending damping C, and its expression is :

$$M_{d,i} = -C_i \Delta\dot\theta_i \quad (13)$$

Its potential function is called the Rayleigh dissipation function D:

$$D = \frac{1}{2}\left(\sum_{i=1}^{n} C_i(\dot\theta_i - \dot\theta_{i-1})^2\right) \quad (14)$$

D. Morison forces

These forces characterize the interaction between the moving fluid (water) around the structure and the structure. They are valid for slender cylinder, which means in the present study that the diameter of the pipe should be significantly smaller than the swell wavelength [8](12.2).

These forces are divided into two terms: a force linked to speed, drag, and a force proportional to acceleration, inertia.

Drag force is a non conservative force because it dissipates the energy of the system.

It is proportional to the square of the relative velocity between the fluid and the body, whose expression is the following :

$$\vec{v_{rel_i}} = \begin{pmatrix} v_{f_{x,i}} - \dot x_i \\ v_{f_{z,i}} - \dot z_i \end{pmatrix}\begin{pmatrix} \vec{e_x} \\ \vec{e_z} \end{pmatrix} = \begin{pmatrix} v_{rel_{x,i}} \\ v_{rel_{z,i}} \end{pmatrix}\begin{pmatrix} \vec{e_x} \\ \vec{e_z} \end{pmatrix} \quad (15)$$

With $\vec{e_{\theta_i}}$ and $\vec{e_{r_i}}$ being respectively the transversal unity vector and the longitudinal unity vector in the local referential illustrated by the figure 5.

$\vec{e_x}$ and $\vec{e_z}$ are expressed in the local referential as follow :

$$\vec{e_x} = \sin\theta_i \vec{e_{r_i}} + \cos\theta_i \vec{e_{\theta_i}}$$
$$\vec{e_z} = -\cos\theta_i \vec{e_{r_i}} + \sin\theta_i \vec{e_{\theta_i}} \quad (16)$$

Fig. 5: Local polar referential

Thus the relative velocity is written in the local referential:

$$\vec{v_{rel_i}} = \begin{pmatrix} v_{rel_{x,i}}\sin\theta_i - v_{rel_{z,i}}\cos\theta_i \\ v_{rel_{x,i}}\cos\theta_i + v_{rel_{z,i}}\sin\theta_i \end{pmatrix}\begin{pmatrix} \vec{e_{r_i}} \\ \vec{e_{\theta_i}} \end{pmatrix} \quad (17)$$

As the angles θ are small, the longitudinal drag component is neglected. Therefore, the considered drag force is fully transversal and proportional to the square of the transversal relative velocity:

$$\vec{v_{rel_{\theta_i}}} = (v_{rel_{x,i}}\cos\theta_i + v_{rel_{z,i}}\sin\theta_i)\vec{e_{\theta_i}} \quad (18)$$

The transversal drag force is expressed as follow :

$$\vec{F_{D_i}} = \frac{1}{2}\rho_i C_{D_i} S_i |v_{rel_{\theta_i}}| \vec{v_{rel_{\theta_i}}} \quad (19)$$

➢ <u>Loop design</u>

- Continuous optimization
- Design improvement
- Product adaptation
- Tailored tools

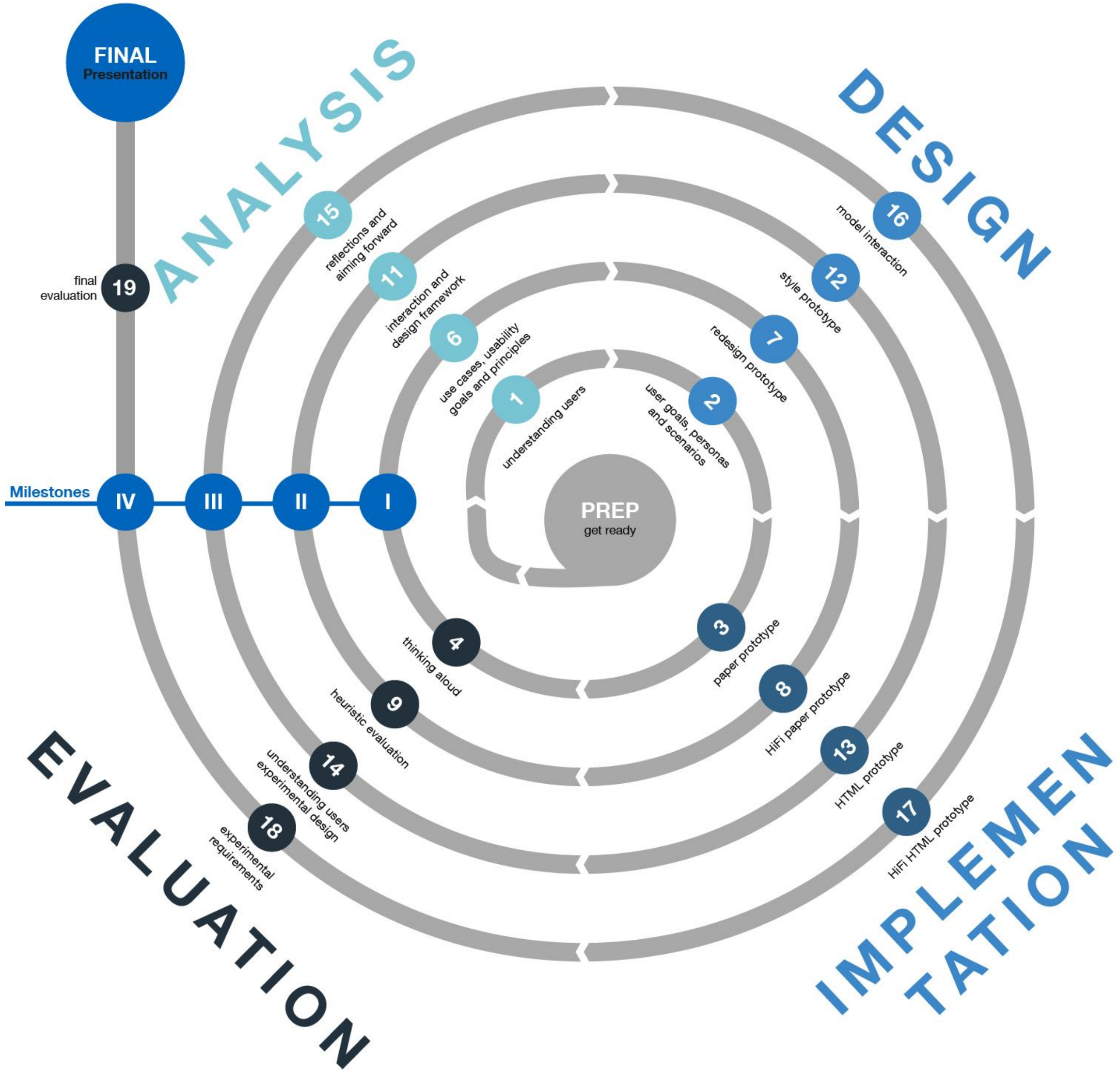

THANK YOU
FOR YOUR ATTENTION

lowtech solution

www.deeprun.re

Matthieu HOARAU
La Réunion
+262 692 92 45 45
matthieu.hoarau@deeprun.re

Lucas VATINEL
Marseille
+33 7 86 41 18 97
lucas.vatinel@deeprun.re

Ludovic MOUTIEN
La Réunion
+33 6 17 01 88 19
ludovic.moutien@deeprun.re